Evidence for Short-Range-Ordered Charge Stripes Far above the Charge-Ordering Transition in $La_{1.67}Sr_{0.33}NiO_4$

A. M. Milinda Abeykoon,[1] Emil S. Božin,[1] Wei-Guo Yin,[1] Genda Gu,[1] John P. Hill,[1] John M. Tranquada,[1] and Simon J. L. Billinge[1,2]

[1]*Condensed Matter Physics and Materials Science Department, Brookhaven National Laboratory, Upton, New York 11973, USA*
[2]*Department of Applied Physics and Applied Mathematics, Columbia University, New York, New York 10027, USA*

(Received 31 May 2013; revised manuscript received 17 July 2013; published 30 August 2013)

The temperature evolution of structural effects associated with charge order (CO) and spin order in $La_{1.67}Sr_{0.33}NiO_4$ has been investigated using neutron powder diffraction. We report an anomalous shrinking of the c/a lattice parameter ratio that correlates with T_{CO}. The sign of this change can be explained by the change in interlayer Coulomb energy between the static-stripe-ordered state and the fluctuating-stripe-ordered state or the charge-disordered state. In addition, we identify a contribution to the mean-square displacements of Ni and in-plane O atoms whose width correlates quite well with the size of the pseudogap extracted from the reported optical conductivity, with a non-Debye-like component that persists below and well above T_{CO}. We infer that dynamic charge-stripe correlations survive to $T \sim 2T_{CO}$.

DOI: 10.1103/PhysRevLett.111.096404 PACS numbers: 71.27.+a, 61.05.F−, 71.45.Lr, 74.72.Kf

The phenomenology of charge and spin stripes has been of considerable interest in a broad range of strongly correlated electron systems [1–6], and in particular with regard to the problem of high-temperature superconductivity in cuprates [7–9]. Although static charge-stripe-order (CO) and spin-order (SO) have been detected by diffraction techniques only in select cuprate materials [10–12], stripe-like modulations of electronic states have been detected at the surface of cleavable cuprates by scanning tunneling spectroscopy [13–15], and a new type of charge correlation has recently been identified in $YBa_2Cu_3O_{6+x}$ [16–20]. When static charge-stripe order occurs in $La_{2-x}Ba_xCuO_4$ [21], it competes with Josephson coupling between the superconducting layers [22–25]. Dynamic stripes may have a broader relevance to superconductivity in the cuprates [26]; however, there is not yet any direct, incontrovertible evidence for dynamic charge stripes in cuprates.

$La_{2-x}Sr_xNiO_4$ has served as a model system for studying stripe order [27]. Charge-stripe order can occur at relatively high temperatures, reaching a maximum of $T_{CO} = 240$ K at $x = 1/3$ [28,29]. While the stripe order is more classical than in the cuprates, with quantum fluctuations being unimportant, there is the possibility that dynamical stripes might exist above T_{CO}. Inelastic neutron scattering studies have already shown that spin-stripe correlations survive above both T_{SO} and T_{CO} [30]. An x-ray scattering study was able to follow critical scattering associated with charge-stripe correlations to temperatures slightly above T_{CO}, but ran out of signal by $T_{CO} + 20$ K [31]. In contrast, measurements of optical conductivity have demonstrated the absence of a dominant Drude peak, the signature of a conventional metallic state, to temperatures as high as $2T_{CO}$ [32]. The fact that the optical conductivity remains peaked at finite frequency suggests that the charge carriers are quasilocalized, which might be the result of fluctuating charge stripes persisting at high temperature.

In this Letter, we use neutron scattering from a polycrystalline sample to investigate the structural response associated with charge-stripe correlations in $La_{1.67}Sr_{0.33}NiO_4$ (LSNO). This might appear to be a surprising approach, as even in the stripe-ordered state the superlattice peaks associated with stripe order are too weak to detect by powder diffraction. Nevertheless, we observe distinct signatures in the temperature-dependent scattering associated with the loss of static charge stripe order at T_{CO} and the gradual attenuation of fluctuating stripes at much higher temperatures.

The $La_{1.67}Sr_{0.33}NiO_4$ sample studied here was initially prepared as a single crystal by the traveling-solvent floating-zone method; a portion of the crystal was then ground to powder form. Neutron diffraction measurements on a piece of the starting crystal have confirmed that $T_{CO} = 240$ K, consistent with previous work [28,29,31]. Time-of-flight neutron powder diffraction measurements were carried out at the NPDF beam line [33] of the Los Alamos Neutron Scattering Center at Los Alamos National Laboratory. Data were converted to the pair distribution function (PDF) using PDFgetN [34] and the PDF was modeled using PDFgui [35]. Rietveld refinements were performed using GSAS+EXPGUI [36,37]. The tetragonal space group $I4/mmm$ was used in the refinements [38]. More details of the experiments and data reduction may be found in the Supplemental Material [39].

Representative Rietveld and PDF fits to the 80 K data are shown in Fig. 1. The model fit to the data is the undistorted tetragonal structure, which does not allow for the average atomic displacements associated with charge ordering. The fits are good, which indicates that any structural modification due to the charge ordering is small, consistent with

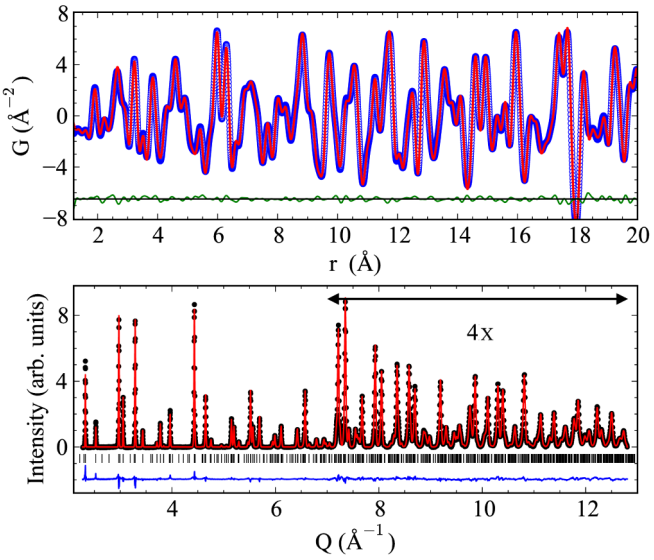

FIG. 1 (color online). PDF (top) and Rietveld (bottom) fits to 80 K data. In both panels, structure models are shown as red solid lines, while the data are shown as circles. Difference curves are offset for clarity.

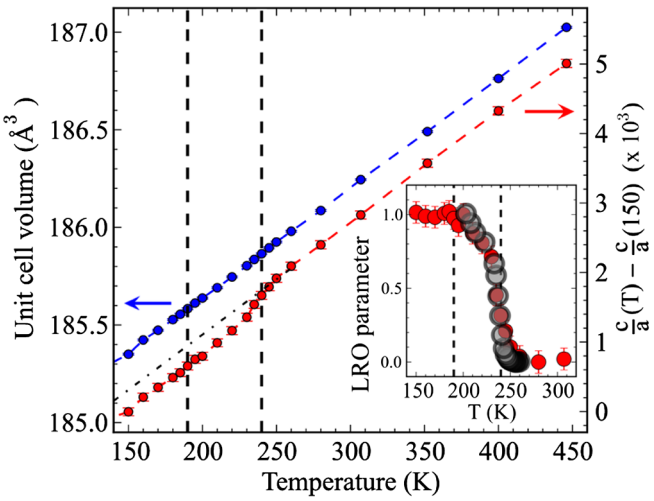

FIG. 2 (color online). The temperature evolution of c/a ratio (bottom curve with red solid circles) in comparison with the volume expansion (top curve with blue solid circles). Dotted lines indicate $T_{SO} = 190$ K and $T_{CO} = 240$ K. In the inset, the red solid circles represent a normalized long-range-order (LRO) parameter calculated from c/a, and the black open circles represents the T evolution of the normalized integrated intensity of the single crystal CO peak from Du *et al.* [31].

earlier studies [38]. No charge or spin superlattice peaks are evident in the data; even in the best case of a nickelate with 3D long-range order, the superlattice intensities are no more than 10^{-4} relative to strong fundamental reflections [40], which is beyond the dynamic range for powder diffraction. While we do not detect the average atomic displacements associated with charge ordering, the transition is revealed by a modification of the tetragonality of the unit cell. The unit cell volume varies smoothly with temperature, as shown in Fig. 2 by the blue circles, in agreement with earlier studies [41]; however, the c/a ratio exhibits a strong anomaly at T_{CO}. This anomaly results from a contraction in the c and an elongation in the a directions in a way that preserves the total unit cell volume. To the best of our knowledge, this is the first time an anomaly in the LSNO unit cell constants at T_{CO} has been reported. It correlates well with anomalies in the sound velocity [28] and thermal conductivity [42].

We can define an order parameter based on this structural response by quantifying how the c/a ratio deviates from a smooth extrapolation of the high-temperature behavior. We use the T dependence of the unit cell volume for this purpose, which we rescale to lie on top of the c/a curve in the high-temperature region. Taking the difference and normalizing the signal to a jump of unity, the resulting order parameter is shown in the inset of Fig. 2. Plotted with it is the normalized single crystal CO peak intensity [31], which is proportional to the square of the conventional order parameter for the charge-ordering transition. Both show the same T dependence, indicating that the anomaly in c/a originates from the development of long-range charge order.

The observed charge stripes in the low-T phase of LSNO for $x = 1/3$ lie in the NiO_2 plane and are diagonal with respect to the nearest neighbor nickel ions. This pattern of charge order is consistent with the Wigner-crystal model from electrostatic considerations. It is interesting to examine whether the same considerations could account for the c/a anomaly. To understand how charge ordering may couple to the lattice parameters, we consider three extremes: (1) ordered stripes, with a staggered stacking as observed experimentally, (2) ordered stripes, without any stacking order along the c axis, and (3) uniform charge in layers. Evaluating the interlayer Coulomb energy for these three configurations, we find that minimization of the Coulomb energy is consistent with an anomalous reduction of the c/a ratio at T_{CO}. (Details are presented in the Supplemental Material [39].)

We now turn our attention to the local structure. Atomic displacements associated with charge stripes, whether static or dynamic, should contribute to measures of disorder relative to the tetragonal model. From the Rietveld refinement of the diffraction pattern, we obtain atomic displacement parameters (ADPs), where the ADP for a particular atomic site in the unit cell can be written as $U_{ii} = \langle u_i^2 \rangle$, where u_i is the instantaneous displacement of such an atom along direction i and the average is over time and configuration. In the PDF, disorder will impact the widths of contributions for individual interatomic distributions (although these may overlap and interfere). For well-behaved materials, the temperature dependence of the ADPs is well explained [43] by the simple Debye model [44]. Deviations from this behavior may indicate the appearance of underlying structural distortions [45,46]. The temperature-dependent anisotropic ADPs

from various atoms in the LSNO structure obtained from Rietveld refinements are shown in Fig. 3. The thermal evolution of various other ADPs are shown in Fig. 3(a) while the ADPs that lie along in-plane nickel-oxygen bonds are shown in Fig. 3(b). In each case the dashed lines (not vertical) represent Debye-model fits to the low-temperature region of the data (with an explanation of the Debye model given in the Supplemental Material [39]). The directions of the different ADPs are indicated in the inset of Fig. 3(a).

For the examples in Fig. 3(a), the measured ADPs lie on, or close to, the Debye curves at all temperatures, suggesting that the behavior is dominated by conventional disorder due to harmonic motion. The ADPs for oxygen atoms in directions perpendicular to the Ni-O bonds, O_a U_{11} and O_p U_{33}, are significantly larger in amplitude than the other ADPs in Fig. 3(a), yielding lower Debye temperatures in the fits, suggesting lower-energy rotational motions of the NiO_6 octahedra, as expected in structures based on the perovskite motif, and as noted before.

In contrast, the ADPs for the in-plane O and Ni atoms in directions *parallel* to the in-plane Ni-O bonds, shown in Fig. 3(b), exhibit large deviations from conventional behavior. These ADPs are the ones we anticipate should have substantial contributions associated with stripe order below T_{CO} [40]. Each ADP should involve a sum of two contributions, one from the stripe-related displacements and another from the usual vibrational motion. Indeed, we see that the ADPs asymptotically approach a Debye curve at high temperature. We infer that the excess magnitude of each ADP above the shifted Debye curve (dotted lines) is associated with stripe correlations. Intriguingly, there is no dramatic change at T_{CO} where static stripe order disappears. Instead, the low-temperature behavior can be characterized by a distinct Debye curve, with downward deviations beginning near the T_{SO}. The stripe-related disorder above T_{CO} is presumably dynamic, given the effective disappearance of elastic diffuse scattering in single-crystal neutron-scattering experiments.

We can define a measure of local stripe correlations as

$$\Delta(T) = \sqrt{U^A_{ii}(T)} - \sqrt{U^A_{D_{ii}}(T)}, \quad (1)$$

where A indicates the atomic species and $U_{D_{ii}}$ represents the Debye approximation to the high-temperature behavior. The "order" parameters from in-plane Ni U_{11} and O U_{22}, normalized to unity, are shown in the inset of Fig. 3(b). There is essentially identical temperature dependence for the Ni and O sites.

To make a connection with the electronic properties, one can compare the temperature dependence of the local order parameters with the optical conductivity data from Katsufuji *et al.* [32]. The energy gap for finite conductivity closes at T_{CO}, but this provides no measure of the correlations that survive above T_{CO}. To better capture the effective pseudogap, we have evaluated the energy at which the

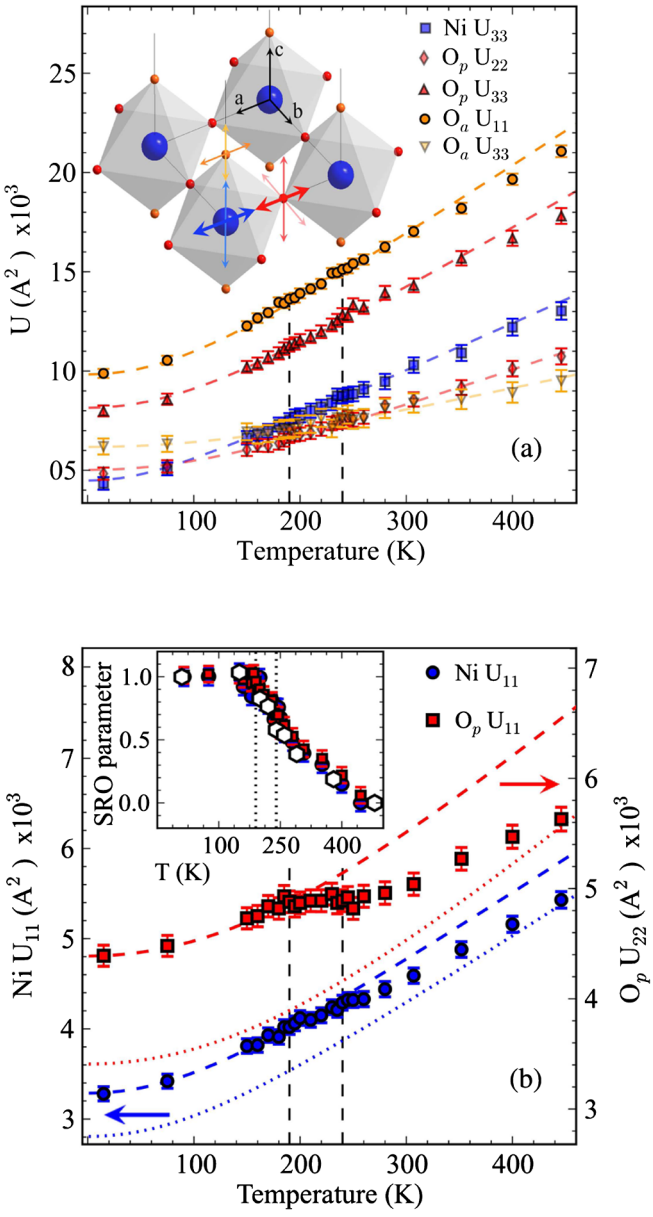

FIG. 3 (color online). Anisotropic ADPs that are not along in-plane Ni-O bonds are shown in (a), while the ADPs that lie along these bonds are shown in (b). The structure is shown in the inset of (a) to illustrate the atoms and the directions of the different anisotropic ADPs that are plotted in the main panels, with Ni in blue, apical oxygen (O_a) in orange, and in-plane oxygen (O_p) in red. Vertical dotted lines indicate the spin- and charge-ordering temperatures, T_{SO} and T_{CO}. Dashed lines represent calculated Debye behavior. The dotted lines in (b) represent calculated Debye behavior with different offsets that are appropriate to fit the high-T ADPs. The inset contains the same ADP data converted to a short-range-order (SRO) parameter, which is the normalized difference from the high-T Debye fit as described in the text, where the symbols used are the same as in the main panel. Plotted on top is a similar SRO parameter for the energy of the pseudogap as determined from optical conductivity measurements as described in the text.

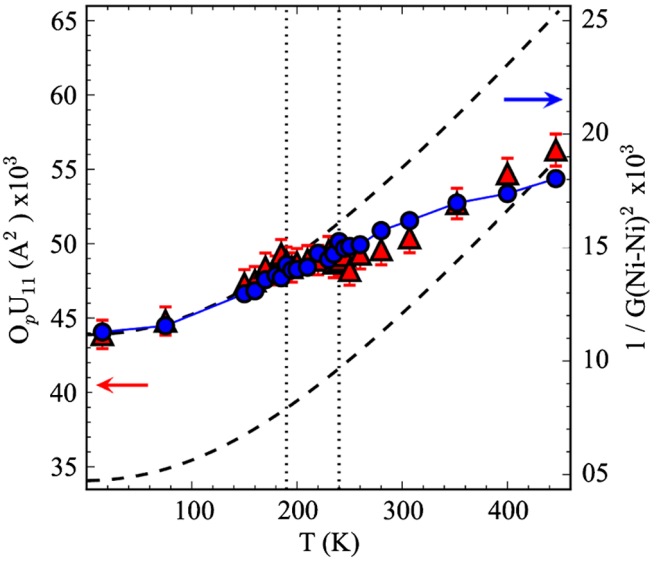

FIG. 4 (color online). Comparison of the temperature evolution of the squared inverse height of the nearest neighbor Ni-Ni PDF peak (blue solid circles) and of the in-plane oxygen U_{22} (red triangles).

optical conductivity falls to half of its peak value at each temperature. With normalization at low temperature, this quantity is plotted in the inset of Fig. 3(b) using open symbols. A remarkable resemblance is observed between the local order parameters from the ADPs and the temperature evolution of the energy gap, which directly links the pseudogap behavior in LSNO and the presence of stripe correlations in the local structure.

The local structural response can also be extracted from PDF analysis. To keep the analysis simple, we focus on just the correlations for atoms separated by the a lattice parameter (3.83 Å), corresponding to the near-neighbor O-O distance that also includes Ni-Ni neighbors. The area of this peak stays essentially constant with temperature, but the width varies. The inverse square PDF peak height is proportional to the square width, or ADP, of that correlation and so is a sensitive and model-independent way of interrogating the data for this parameter. The temperature evolution of the inverse square PDF peak height is shown in Fig. 4 as blue solid circles. For comparison, the in-plane oxygen ADP along the Ni-O bond, U_{22}, is indicated by red triangles. The inverse square PDF peak height shows the same T dependence. A clear break in slope can be observed in the T evolution of the inverse square PDF peak height at T_{SO}, indicating its sensitivity to stripe order, and the behavior closely follows the Rietveld ADP for the in-plane oxygen along the bond. Thus, the PDF, which is a model-independent complementary measure of the evolution of CO, confirms the Rietveld result.

In summary, we have presented a temperature-dependent neutron powder diffraction study of LSNO, which is known to show robust charge-stripe order below 240 K. We have shown that the tetragonality shows an anomalous change at T_{CO}. In contrast, a local order parameter determined from mean-square displacements of Ni and in-plane O sites, or equivalently from squared PDF peak widths, shows a temperature dependence that correlates quite well with the pseudogap in the optical conductivity [32]. From this behavior, we have inferred that charge-stripe correlations survive to temperatures far above T_{CO}, and only gradually become attenuated. These results provide support for the idea that short-range-ordered, and presumably fluctuating, stripes could underlie electronic features, such as pseudogap and nematic and smectic phases seen in the related cuprates [26,47].

This work was supported by the Office of Basic Energy Sciences, Division of Materials Sciences and Engineering, U.S. Department of Energy through account No. DE-AC02-98CH10886. This work has benefited from the use of NPDF at LANSCE, funded by DOE Office of Basic Energy Sciences. LANL is operated by Los Alamos National Security LLC under DOE Contract No. DE-AC52-06NA25396.

[1] N. Ikeda, H. Ohsumi, K. Ohwada, K. Ishii, T. Inami, K. Kakurai, Y. Murakami, K. Yoshii, S. Mori, Y. Horibe, and H. Kito, Nature (London) **436**, 1136 (2005).
[2] M. Coey, Nature (London) **430**, 155 (2004).
[3] M. S. Senn, J. P. Wright, and J. P. Attfield, Nature (London) **481**, 173 (2012).
[4] H. Ulbrich and M. Braden, Physica (Amsterdam) **481C**, 31 (2012).
[5] M. Hücker, Physica (Amsterdam) **481C**, 3 (2012).
[6] T. Wu, H. Mayaffre, S. Kramer, M. Horvatic, C. Berthier, W. N. Hardy, R. Liang, D. A. Bonn, and M.-H. Julien, Nature (London) **477**, 191 (2011).
[7] S. A. Kivelson, I. P. Bindloss, E. Fradkin, V. Oganesyan, J. M. Tranquada, A. Kapitulnik, and C. Howald, Rev. Mod. Phys. **75**, 1201 (2003).
[8] M. Vojta, Adv. Phys. **58**, 699 (2009).
[9] J. Zaanen, O. Y. Osman, H. V. Kruis, Z. Nussinov, and J. Tworzydło, Philos. Mag. B **81**, 1485 (2001).
[10] M. Hücker, Physica (Amsterdam) **481C**, 3 (2012).
[11] P. Abbamonte, E. Demler, J. S. Davis, and J.-C. Campuzano, Physica (Amsterdam) **481C**, 15 (2012).
[12] M. Fujita, Physica (Amsterdam) **481C**, 23 (2012).
[13] J. A. Robertson, S. A. Kivelson, E. Fradkin, A. C. Fang, and A. Kapitulnik, Phys. Rev. B **74**, 134507 (2006).
[14] Y. Kohsaka, C. Taylor, K. Fujita, A. Schmidt, C. Lupien, T. Hanaguri, M. Azuma, M. Takano, H. Eisaki, H. Takagi, S. Uchida, and J. C. Davis, Science **315**, 1380 (2007).
[15] C. V. Parker, P. Aynajian, E. H. da Silva Neto, A. Pushp, S. Ono, J. Wen, Z. Xu, G. Gu, and A. Yazdani, Nature (London) **468**, 677 (2010).
[16] G. Ghiringhelli, M. Le Tacon, M. Minola, S. Blanco-Canosa, C. Mazzoli, N. B. Brookes, G. M. De Luca, A. Frano, D. G. Hawthorn, F. He, T. Loew, M. M. Sala, D. C. Peets, M. Salluzzo, E. Schierle, R. Sutarto, G. A. Sawatzky, E. Weschke, B. Keimer, and L. Braicovich, Science **337**, 821 (2012).

[17] J. Chang, E. Blackburn, A. T. Holmes, N. B. Christensen, J. Larsen, J. Mesot, R. Liang, D. A. Bonn, W. N. Hardy, A. Watenphul, M. v. Zimmermann, E. M. Forgan, and S. M. Hayden, Nat. Phys. **8**, 871 (2012).
[18] E. Blackburn, J. Chang, M. Hücker, A. T. Holmes, N. B. Christensen, R. Liang, D. A. Bonn, W. N. Hardy, U. Rütt, O. Gutowski, M. v. Zimmermann, E. M. Forgan, and S. M. Hayden, Phys. Rev. Lett. **110**, 137004 (2013).
[19] S. Blanco-Canosa, A. Frano, T. Loew, Y. Lu, J. Porras, G. Ghiringhelli, M. Minola, C. Mazzoli, L. Braicovich, E. Schierle, E. Weschke, M. Le Tacon, and B. Keimer, Phys. Rev. Lett. **110**, 187001 (2013).
[20] V. Thampy, S. Blanco-Canosa, M. García-Fernández, M. P. M. Dean, G. D. Gu, M. Föerst, B. Keimer, M. Le Tacon, S. B. Wilkins, and J. P. Hill, Phys. Rev. B **88**, 024505 (2013).
[21] M. Hücker, M. v. Zimmermann, G. D. Gu, Z. J. Xu, J. S. Wen, G. Xu, H. J. Kang, A. Zheludev, and J. M. Tranquada, Phys. Rev. B **83**, 104506 (2011).
[22] S. Tajima, T. Noda, H. Eisaki, and S. Uchida, Phys. Rev. Lett. **86**, 500 (2001).
[23] Q. Li, M. Hücker, G. D. Gu, A. M. Tsvelik, and J. M. Tranquada, Phys. Rev. Lett. **99**, 067001 (2007).
[24] E. Berg, E. Fradkin, S. A. Kivelson, and J. M. Tranquada, New J. Phys. **11**, 115004 (2009).
[25] C. C. Homes, M. Hücker, Q. Li, Z. J. Xu, J. S. Wen, G. D. Gu, and J. M. Tranquada, Phys. Rev. B **85**, 134510 (2012).
[26] S. A. Kivelson, E. Fradkin, and V. J. Emery, Nature (London) **393**, 550 (1998).
[27] H. Ulbrich and M. Braden, Physica (Amsterdam) **481C**, 31 (2012).
[28] A. P. Ramirez, P. L. Gammel, S.-W. Cheong, D. J. Bishop, and P. Chandra, Phys. Rev. Lett. **76**, 447 (1996).
[29] S.-H. Lee and S.-W. Cheong, Phys. Rev. Lett. **79**, 2514 (1997).
[30] S.-H. Lee, J. M. Tranquada, K. Yamada, D. J. Buttrey, Q. Li, and S.-W. Cheong, Phys. Rev. Lett. **88**, 126401 (2002).
[31] C.-H. Du, M. E. Ghazi, Y. Su, I. Pape, P. D. Hatton, S. D. Brown, W. G. Stirling, M. J. Cooper, and S.-W. Cheong, Phys. Rev. Lett. **84**, 3911 (2000).
[32] T. Katsufuji, T. Tanabe, T. Ishikawa, Y. Fukuda, T. Arima, and Y. Tokura, Phys. Rev. B **54**, R14 230 (1996).
[33] T. Proffen, T. Egami, S. J. L. Billinge, A. K. Cheetham, D. Louca, and J. B. Parise, Appl. Phys. A **74**, s163 (2002).
[34] P. F. Peterson, M. Gutmann, T. Proffen, and S. J. L. Billinge, J. Appl. Crystallogr. **33**, 1192 (2000).
[35] C. L. Farrow, P. Juhás, J. Liu, D. Bryndin, E. S. Božin, J. Bloch, T. Proffen, and S. J. L. Billinge, J. Phys. Condens. Matter **19**, 335219 (2007).
[36] A. C. Larson and R. B. Von Dreele, Los Alamos National Laboratory Report No. LAUR-86-748, 2004.
[37] B. H. Toby and S. J. L. Billinge, Acta Crystallogr. Sect. A **60**, 315 (2004).
[38] G. Wu, J. J. Neumeier, C. D. Ling, and D. N. Argyriou, Phys. Rev. B **65**, 174113 (2002).
[39] See Supplemental Material at http://link.aps.org/supplemental/10.1103/PhysRevLett.111.096404 for a description of the sample preparation method, neutron powder diffraction measurements, and the details of the theory used in the main text to explain the results. The Supplemental Material also contains a plot of the bond length ratio, (Ni-Oa)/(Ni-Op).
[40] J. M. Tranquada, J. E. Lorenzo, D. J. Buttrey, and V. Sachan, Phys. Rev. B **52**, 3581 (1995).
[41] G. Wu, J. J. Neumeier, C. D. Ling, and D. N. Argyriou, Phys. Rev. B **65**, 174113 (2002).
[42] C. Hess, B. Büchner, M. Hücker, R. Gross, and S.-W. Cheong, Phys. Rev. B **59**, R10 397 (1999).
[43] S. J. L. Billinge, P. K. Davies, T. Egami, and C. R. A. Catlow, Phys. Rev. B **43**, 10 340 (1991).
[44] P. Debye, Ann. Phys. (Berlin) **344**, 789 (1912).
[45] S. J. L. Billinge, R. G. DiFrancesco, G. H. Kwei, J. J. Neumeier, and J. D. Thompson, Phys. Rev. Lett. **77**, 715 (1996).
[46] E. S. Božin, C. D. Malliakas, P. Souvatzis, T. Proffen, N. A. Spaldin, M. G. Kanatzidis, and S. J. L. Billinge, Science **330**, 1660 (2010).
[47] M. J. Lawler, K. Fujita, J. Lee, A. R. Schmidt, Y. Kohsaka, C. K. Kim, H. Eisaki, S. Uchida, J. C. Davis, J. P. Sethna, and E.-A. Kim, Nature (London) **466**, 347 (2010).